URSI AP-RASC, Sydney, Australia, 17 – 22 August 2025

A Novel mm-Wave Hybrid Beamformer-Based Integrated Sensing and Communication Testbed

Yunsong Gui* (1), Hamid Amiriara(2), Mahtab Mirmohseni(2), Mohsen Khalily(2), Rahim Tafazolli(2) and Tian Hong Loh(1)
(1) National Physical Laboratory, Teddington, Middlesex TW11 0LW, United Kingdom
(2) Institute for Communication Systems, University of Surrey, Guildford GU2 7XS, United Kingdom

Abstract

This paper presents an innovative testbed for integrated sensing and communication (ISAC) applications. We propose a fully functional millimeter-wave (mm-wave) bi-static ISAC testbed, comprising a mm-wave hybrid beamformer-based signal generator at the transmitter (TX) side and a phase-coherent multi-channel digital beamformer at the receiver (RX) side. The testbed features a highly configurable system that includes a mm-wave fully-connected hybrid beamformer incorporated with a user-programmable software-defined radio (SDR) platform. This configuration offering enhanced flexibility for optimizing dual-functional system design and mitigating mutual interference in ISAC systems. Several techniques such as multi-channel self-calibration at the receiver and beam weighting optimization at the transmitter, are implemented to ensure optimal ISAC performance. Finally, initial performance validation of the testbed is demonstrated through real-world measurements focusing on a typical ISAC use case, namely object detection within a fully anechoic chamber.

1. Introduction

Integrated sensing and communication (ISAC), as an emerging candidate technology for sixth generation (6G) mobile networks, has gained increasing attention due to its potential to improve spectrum efficiencies and reduce hardware costs by integrating wireless communication and radar sensing into a single system. However, researchers have identified several key technical challenges that hinder their evolution into a standardized technology. These challenges include the trade-offs in system and waveform design between sensing and communication performance, interference and coexistence issues, and scenarios involving multiple targets and communication users [1, 2].

In terms of ISAC system design, the sensing component typically requires extremely wide bandwidth to achieve high-resolution delay estimation, as well as precise synchronization and phase coherence for accurate spatial parameter estimation. In contrast, the communication component focuses more on waveform design to fully utilize the narrower frequency bands and generally requires less stringent multi-channel synchronization [3]. Technologies such as spectrum sharing, dynamic resource allocation, and dual-functional waveform design are potential solutions for optimizing these trade-offs in ISAC system design [3].

Current trends in developing cost-effective and energy-efficient wireless systems operating at millimeter-wave (mm-wave) frequencies and with large-scale phased array antennas for fulfilling the high data-rate demands of 6G have driven the need to explore the use of hybrid beamforming technologies in ISAC systems, providing significant flexibility in the space domain. Thanks to its high degree of control over phase and amplitude, particularly in fully connected hybrid beamformers [4], key advantages of realizing hybrid beamforming technologies in ISAC systems include, for example:

- Large-scale phased array enables the generation of narrow, steerable beams, allowing for highly precise angle of departure (AoD) estimation;
- Multiple beams with customizable synthesis patterns can be generated to reduce mutual interference between sensing and communication links;
- An additional degree of freedom in the spatial domain provides further flexibility for dynamic ISAC resource allocation.

In this paper, we present our recent work on the design of an ISAC testbed, featuring a fully connected mm-wave hybrid beamformer and its associated key technologies. The rest of the paper is organized as follows: Section 2 provides a general overview of the testbed, Section 0 discusses several critical implementation technologies, including multi-channel synchronization and calibration methods, and Section 4 presents the testbed validation through real-world object detection measurements. Finally, Section 5 concludes the paper.

2. The mm-Wave ISAC Testbed

The proposed mm-wave ISAC testbed is designed to evaluate various ISAC core algorithms and their wireless performance under typical ISAC scenarios in real-world environments. It features a highly flexible architecture to support reconfigurable settings for diverse scenarios. The entire testbed operates within the 26 GHz frequency band, which is typical for the 3rd Generation Partnership Project (3GPP) frequency range 2 (FR2). The system schematic is depicted in Figure 1.

In this paper, a state-of-the-art mm-wave fully-connected beamformer system is incorporated with high-performance

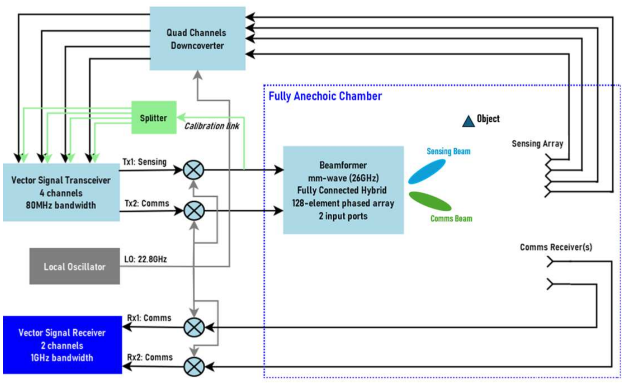

Figure 1. Schematic of the mm-wave beamformer-based ISAC testbed measurement setup.

SDR instrumentation and a pair of custom-designed mm-wave upconverters to form the ideal transmit node for the ISAC system. This configuration generates customizable downlink communication and sensing waveforms. Similarly, the receiving system includes a linear phased array and a frequency-down-conversion multi-channel receiver, which comprise of commercial PXIe vector signal receivers and a quad downconverter.

This setup allows for flexible usage at the receiver (RX) end. Depending on the scenario-oriented signal processing programs, the multi-channel receiver hardware can be easily configured as a digital beamforming system for a sensing receiver or a multiple-input multiple-output (MIMO) receiver for a communication user equipment (UE). Additionally, the testbed includes two extra receiving channels to enhance the capability of the communication links, which can be flexibly configured as a 2-by-2 MIMO UE or two independent single-input single-output (SISO) UEs.

To ensure high-precision synchronization and phase coherency among the multiple RF channels for sensing purposes, a sophisticated synchronization scheme is employed in both transmitter (TX) and RX. This scheme includes shared networks of the local oscillator (LO), reference signals, and trigger signals, for both the intermediate frequency (IF) signal generation and reception across multiple channels, and mm-wave RF signal conversion among all up-converters and down-converters. Furthermore, a separate calibration link is established to estimate and eliminate the inherent initial phase offsets between multiple digital beamforming receive channels, which is further described in Section 3.

Thanks to the high flexibility of the SDR platform, different kinds of ISAC waveforms and algorithms can be developed and evaluated. A typical communication waveform solution, i.e. the 5G New Radio (NR) physical layer protocol, along with a direction of arrival (DoA) algorithm based on the waveform, was developed to evaluate sensing performance under standard 5G waveforms. The performance of the object detection is further described in Section 4.

Table 1. Overview of key specifications for the ISAC testbed.

Specification	Details
Channels setting	TX: 2 RX: 4 (DBF) + 2 (Comms UE)
RF bandwidth	1 GHz for 2 receiving channels 80 MHz for 4 DBF channels Up to 1 GHz for 2 TX and 2 RX
Frequency band	26 GHz
Beamformer array	128-element (16 × 8) microstrip phased array antenna
Beamformer architecture	Hybrid Beamformer (Fully connection architecture)
Configurable phase and amplitude	Fully configurable phase and amplitude for every element
Phase resolution	5.625°
Amplitude resolution	0.5 dB
Beam steering range	-75 degree to 75 degree
Antenna array at Rx	Uniformly linearly placed horn antenna array

3. Key Implementation Technologies

3.1 The mm-wave beamformer

The mm-wave fully connected hybrid beamformer system was presented in [4]. The testbed operates in the 26 GHz mm-wave frequency band, with 2 GHz instantaneous bandwidth, and features a fully configurable attenuator and phase shifter network. This network allows for precise control of the attenuators and phase shifters through a digital input and output (DIO) switch unit. As detailed in Table 1, the 6-bit phase control and 6-bit gain/attenuation control achieve a 5.625° phase resolution and 0.5 dB amplitude resolution, respectively. The beamformer includes a 128-element phased array antenna arranged in a 16 × 8 planar configuration, and two independent RF channels, each capable of fully independent beamforming. Each RF input is split into 16 signals, which are then processed by 16 mm-wave fully connected beamforming modules. Figure 2 provides a detailed diagram of the fully connected network of phase shifters and adjustable attenuators, along with the 128-element TX antenna array.

3.3 Multiple-channel calibration

As previously mentioned, a phase-coherent multi-channel receiver with a signal down-converter was developed and integrated into the ISAC testbed. It consists of two sets of down-converters. The first stage downconverters convert the signals from mm-wave RF 26 GHz to the IF at 3.2 GHz, while the second stage downconverters further convert the IF signal from 3.2 GHz to the baseband. The LO sharing network enables the sharing of LO signals between the multiple channels in both down-conversion stages, ensuring stable phase differences across the channels. Additionally, the reference and trigger-sharing networks ensure coherent timing among the channels. Due to

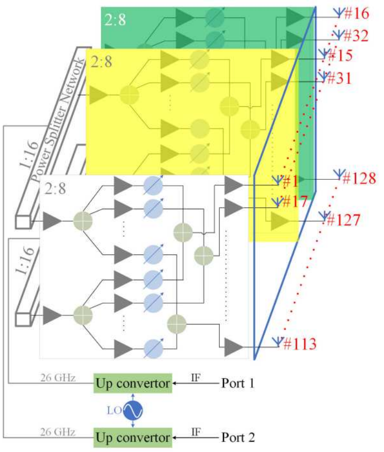

Figure 3. Structure of the fully connected hybrid beamformer [4].

inherent variations in initial phase offsets and timing differences among multiple channels, a time-domain channel sounding-based multichannel calibration method was developed to estimate and eliminate these discrepancies. During calibration, a root-raised cosine (RRC)-filtered Pseudo-Noise (PN) sequence is generated by the sensing channel. Instead of transmitting it through the beamformer, the generated mm-wave signal on the TX side is looped back to the receiving channels via a 1-to-N coupler. After the down-conversion and analog-to-digital (A/D) conversion, a time-domain correlation method is applied to the digitized baseband in-phase and quadrature (IQ) signals to estimate and eliminate phase and timing differences.

Figure 3 demonstrates the calibration results. Figure 3(a) illustrates the estimation of the power delay profile (PDP) after applying the time-domain correlation method to the captured IQ sequences of all receiving channels. Based on the PDP, the phase and integer timing for each channel can be estimated and offsets between multiple channels can be derived. To further estimate timing differences within the sampling period, a phase-frequency-response-based estimation method is designed to obtain the fractional delay, which is shown in Figure 3(b). This method leverages the inherent relationship between delay and the phase frequency response. Figure 3(c) depicts the long-term stability of the multichannel timing and phase discrepancies. After observing a time window of over 30 minutes, the low level of fluctuation confirms the repeatability and effectiveness of the multichannel calibration.

3.2 Beam pattern optimization

According to [5], the synthesized radiation patterns of phased arrays play a crucial role in the ISAC performance, whether for sensing or communication components. For sensing components, the sidelobe of the synthesized radiation pattern of the phased array can significantly reduce the detection dynamic range in sensing applications. To suppress the sidelobe level, a finite impulse response

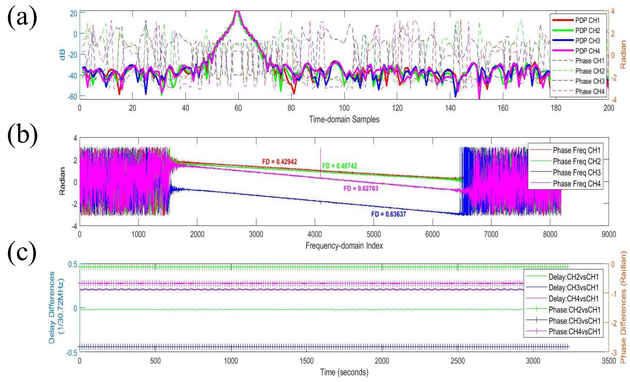

Figure 2. Measurement results of the multi-channel calibration method: (a) phase and integer timing discrepancies, (b) fractional timing differences among multiple channels, and (c) long-term stability of phase and timing discrepancies

(FIR)-filter-based sidelobe suppression algorithm was developed. The 8-order and 16-order FIR filters were designed according to the size of the beamformer phased array in two dimensions. Different sidelobe suppression ratios from 30 to 45 dB, are evaluated as the parameters for the design of filters. Figure 4 shows a gain of approximately 15 dB between the main beam and the maximum sidelobe at the uniform illumination configuration. In the attenuator and amplifier settings, due to the limitations of 0.5 dB resolution and 21.5 dB dynamic range, quantization noise is introduced into the actual beam weighting, reducing the effectiveness of sidelobe suppression, which leads to a maximum 6 dB sidelobe level suppression from the tapped beam weighting.

4. Measurement - Object Detection

To evaluate the performance of the ISAC testbed, an object detection measurement campaign was conducted in a fully anechoic chamber at the National Physical Laboratory (NPL). The NPL small antenna radiated testing (SMART) chamber is 7 m × 6 m × 6 m and is lined with carbon-loaded polyurethane foam absorbers that support frequencies up to 110 GHz. Figure 5 shows the measurement setup in the anechoic chamber. A flat metal plate was used as the object and placed at one end of the

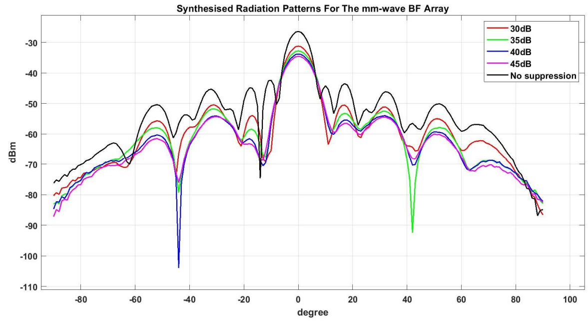

Figure 4. Measured antenna radiation patterns comparing uniform illumination with tapped beam weighting, illustrating the effect of the sidelobe suppression algorithm at various suppression ratios.

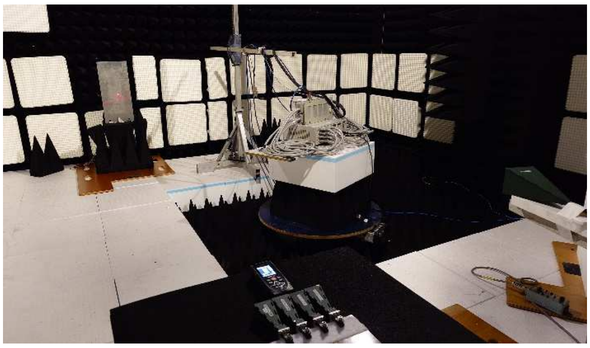

Figure 6. Measurement setup for an object detection

chamber. The distances from the object to the beamformer (TX) and the horn antenna array (RX) were 2.4 m and 4.8 m, respectively.

The 5G NR downlink signal was generated by the beamformer and reached the receiver after being reflected from the object. The waveform parameters are summarized in Table 2. On the TX side, the beamformer continuously steered the beam across the search angle range. On the RX side, a minimum variance distortionless response (MVDR) algorithm was applied to detect the angle of arrival (AoA) of the reflected signal [6]. Figure 6 depicts the joint AoD and AoA spatial spectrum distribution. The estimated AoD was obtained through beam steering at the TX side, while the estimates of AoA were derived using the MVDR estimator at the RX side. The results show that the area with higher power levels in the spatial spectrum closely matches the actual location of the object.

5. Conclusion

In this paper, we presented a novel mm-wave ISAC testbed featuring a fully controllable mm-wave beamformer, a high-precision phase-coherent multi-channel receiver, and a standards-compliant waveform. Several key implementation technologies were introduced to elucidate their roles in enhancing the performance of the testbed. Additionally, preliminary test results on object detection were presented to validate the system's functionality. These results confirm the testbed's capability to integrate and optimize both sensing and communication tasks, marking a significant step forward in the development of technologies for 6G networks. Future work to be considered includes a more comprehensive evaluation of the detection and link performance of the ISAC testbed.

6. Acknowledgements

This work was supported in part by the 2025–2029 National Measurement System Programme of the UK Government's Department for Science, Innovation and Technology (DSIT), Science Theme Reference EMT25, and the UK DSIT under the Future Open Networks Research Challenge project TUDOR (Towards Ubiquitous 3D Open Resilient Network).

Table 2. Downlink waveform parameters for 5G NR signal generation in the ISAC testbed.

Parameter	Value
Sampling rate	30.72 MHz
Subcarrier space	15 kHz
Resource block number	100
Modulation order	QPSK
Downlink format	CP-OFDM
DoA estimation method	MVDR [6]
Beam sweeping range in the azimuth plane	[-20°, 0°] offset from the boresight with a 1° step

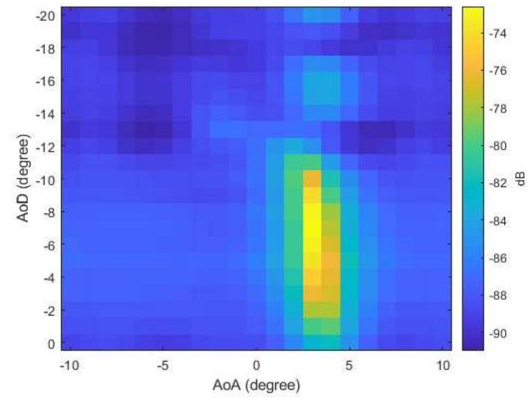

Figure 5. The joint AoD and AoA spectrum analysis

References

[1] S. Lu et al., "Integrated Sensing and Communications: Recent Advances and Ten Open Challenges," *IEEE Internet of Things Journal*, **11**, 11, June 2024, pp. 19094–19120, doi: 10.1109/JIOT.2024.3361173.

[2] H. Amiriara et al., "A Physical Layer Security Framework for Integrated Sensing and Semantic Communication Systems," in Proc. IEEE WCNC, Milan, Italy, 2025, doi: 10.48550/arXiv.2410.06208.

[3] Y. Niu, et al., "Interference Management for Integrated Sensing and Communication Systems: A Survey," *IEEE Internet of Things Journal*, **1**, 1, January 2024, doi: 10.1109/JIOT.2024.3506162.

[4] S. Payami et al., "Developing the First mmWave Fully-Connected Hybrid Beamformer with a Large Antenna Array," *IEEE Access*, **8**, July 2020, pp. 141282–141291, doi: 10.1109/ACCESS.2020.3013539.

[5] R. Zhang et al., "Integrated Sensing and Communication Waveform Design with Sparse Vector Coding: Low sidelobe and Ultra Reliability," *IEEE Transactions on Vehicular Technology*, **71**, 4, April 2022, pp. 4489-4494, doi:10.1109/TVT.2022.3146280.

[6] J. Capon, "High-resolution frequency-wavenumber spectrum analysis", *Proceedings of the IEEE*, **57**, 8, August 1969, pp. 1408–1418, doi: 10.1109/PROC.1969.7278.